Salazar et al. Supplemental Figure 1

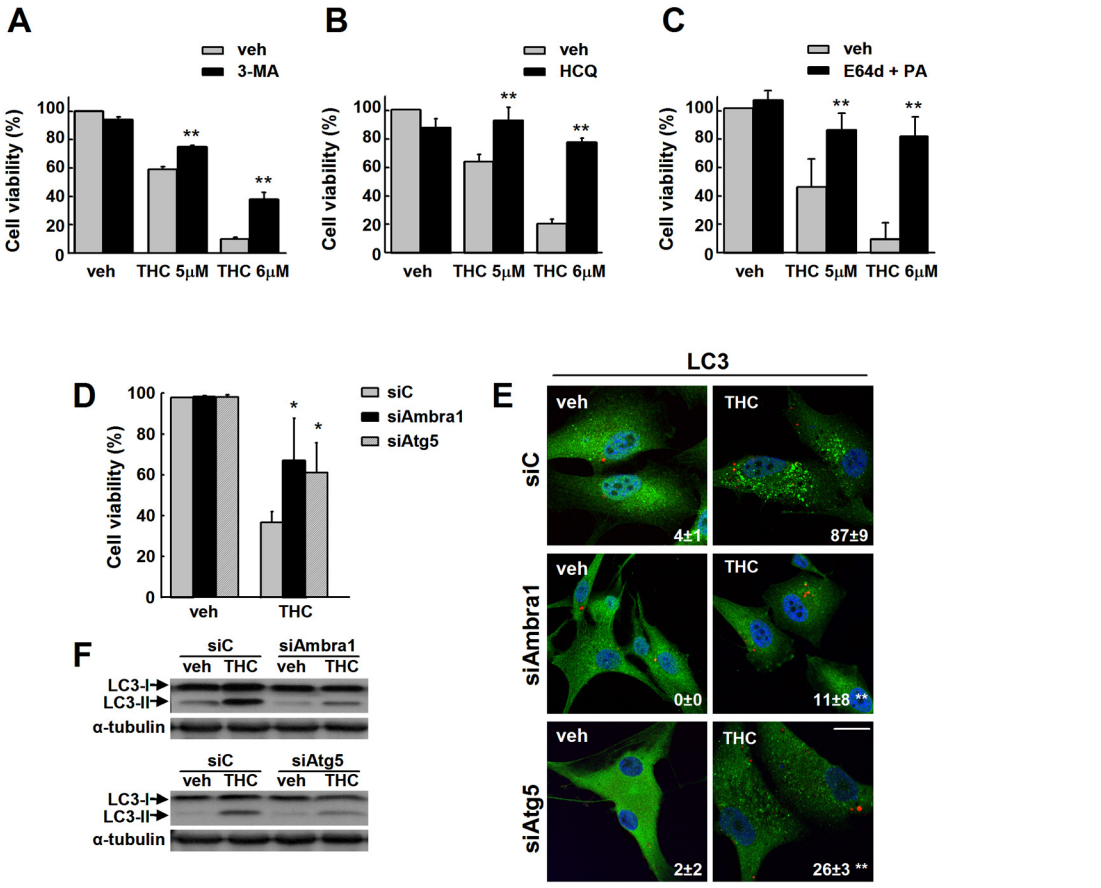

Supplemental Figure 1

Pharmacological and genetic inhibition of autophagy prevents THC-induced cell death. (**A-C**): Effect of THC (24 h) on the viability of U87MG cells pre-incubated with vehicle or 3-MA (5 mM; **A**), hydroxicloroquine (HCQ; 15 μg/ml; **B**) and E64d + PA (10 μM +10 μg/ml; **C**) (mean ± s.d.; n = 10; $*P < 0.05$ or $**P < 0.01$ from THC-treated cells). (**D**) Effect of THC (24 h) on the viability of U87MG cells transfected with siC, siAmbra1 or siAtg5 (mean ± s.d.; n = 5; $*P < 0.05$ from THC-treated siC-transfected cells). Values of gene expression as determined by real-time quantitative PCR (expressed as mean fold change ± s.d. relative to siC-transfected cells; n = 5; $**P < 0.01$ from siC-transfected cells) were 0.3 ± 0.1** and 0.4± 0.1** for siAmbra1- and siAtg5-transfected cells, respectively. (**E**) Effect of THC (18 h) on LC3 immunostaining (green) in U87MG cells transfected with siC, siAmbra1 or siAtg5. Values represent the percentage of cells with LC3 dots relative to the total number of transfected cells (as determined by co-transfection with a red fluorescent control siRNA) (mean ± s.d.; n = 4; $**P < 0.01$ from THC-treated siC-transfected cells). Bar: 20 μm. (**F**) Effect of THC (18 h) on LC3 lipidation in U87MG cells transfected with siC, siAmbra1 or siAtg5 (n = 5).

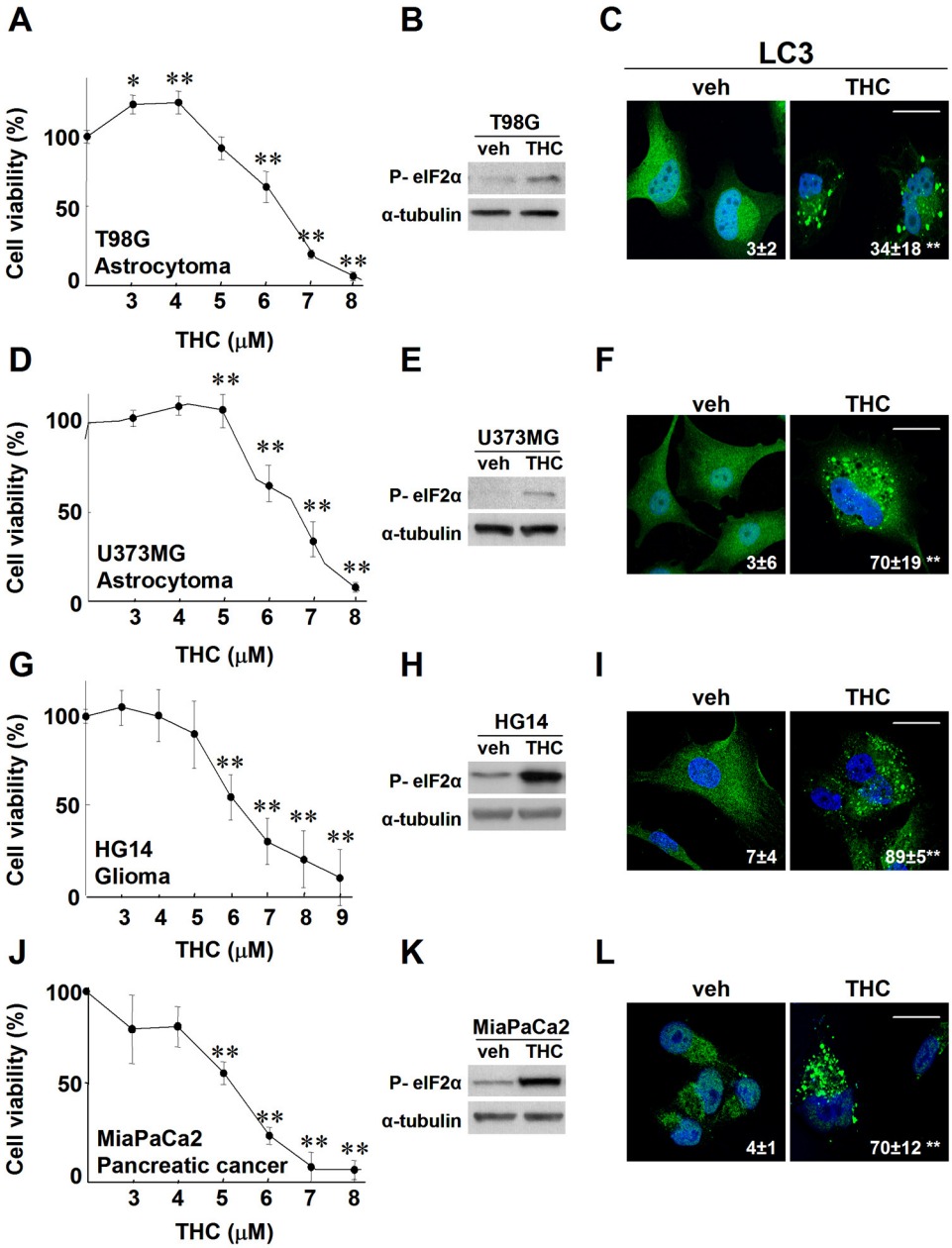

Supplemental Figure 2
THC induces ER-stress, autophagy and cell death in human tumor cells. (**A, D, G. J**) Effect of THC on the viability of T98G (**A**, astrocytoma), U373MG (**D**, astrocytoma), HG14 (**G**, a primary culture derived from a human glioblastoma biopsy), and MiaPaCa2 (**J**, pancreatic cancer) cells (mean ± s.d.; n = 10; **P* < 0.05 or ***P* < 0.01 from vehicle-treated cells). (**B, E, H, K**) Effect of THC on eIF2α phosphorylation of T98G (**B**), U373MG (**E**), HG14 (**H**) and MiaPaCa2 (**K**) cells (3 h; n = 3). (**C, F, I, L**) Effect of THC (18 h) on LC3 immunostaining of T98G (**C**), U373MG (**F**), HG14 (**I**), and MiaPaCa2 (**L**) cells. Values represent the percentage of cells with LC3 dots relative to the total number of cells (mean ± s.d.; n = 3; ***P* < 0.01 from vehicle-treated cells). Bar: 20 μm.

Salazar et al. Supplemental Figure 3

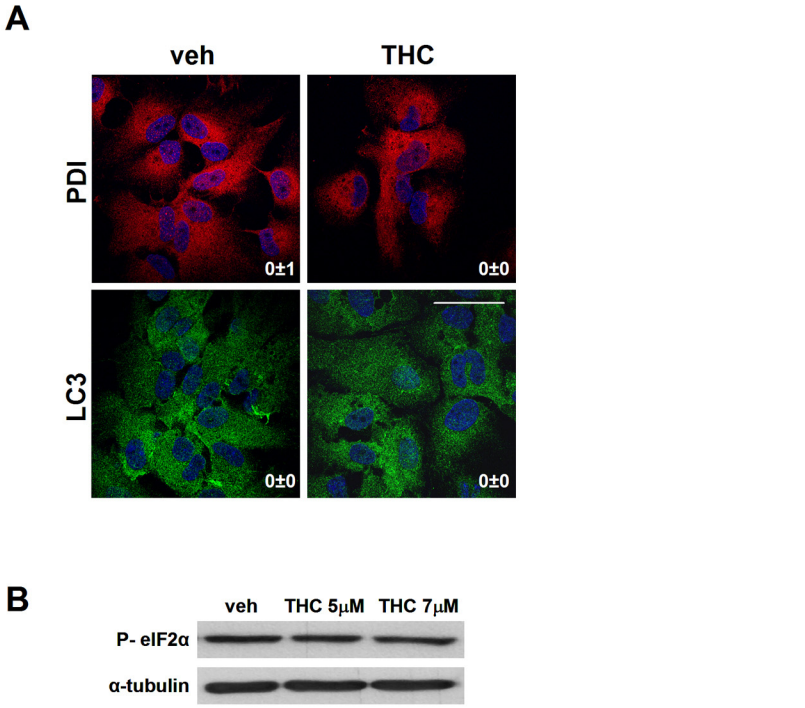

Supplemental Figure 3
Primary astrocytes are resistant to THC-induced ER-stress and autophagy. (**A**) Effect of THC on PDI (8 h) and LC3 (24 h) immunostaining of primary astrocytes (n = 3). Values represent the percentage of cells with PDI (upper photomicrographs) or LC3 (lower photomicrographs) dots relative to the total number of cells (mean ± s.d.; n = 3). Bar: 20 μm. (**B**) Effect of THC on eIF2α phosphorylation of primary astrocytes (3 h; n = 3).

Salazar et al. Supplemental Figure 4

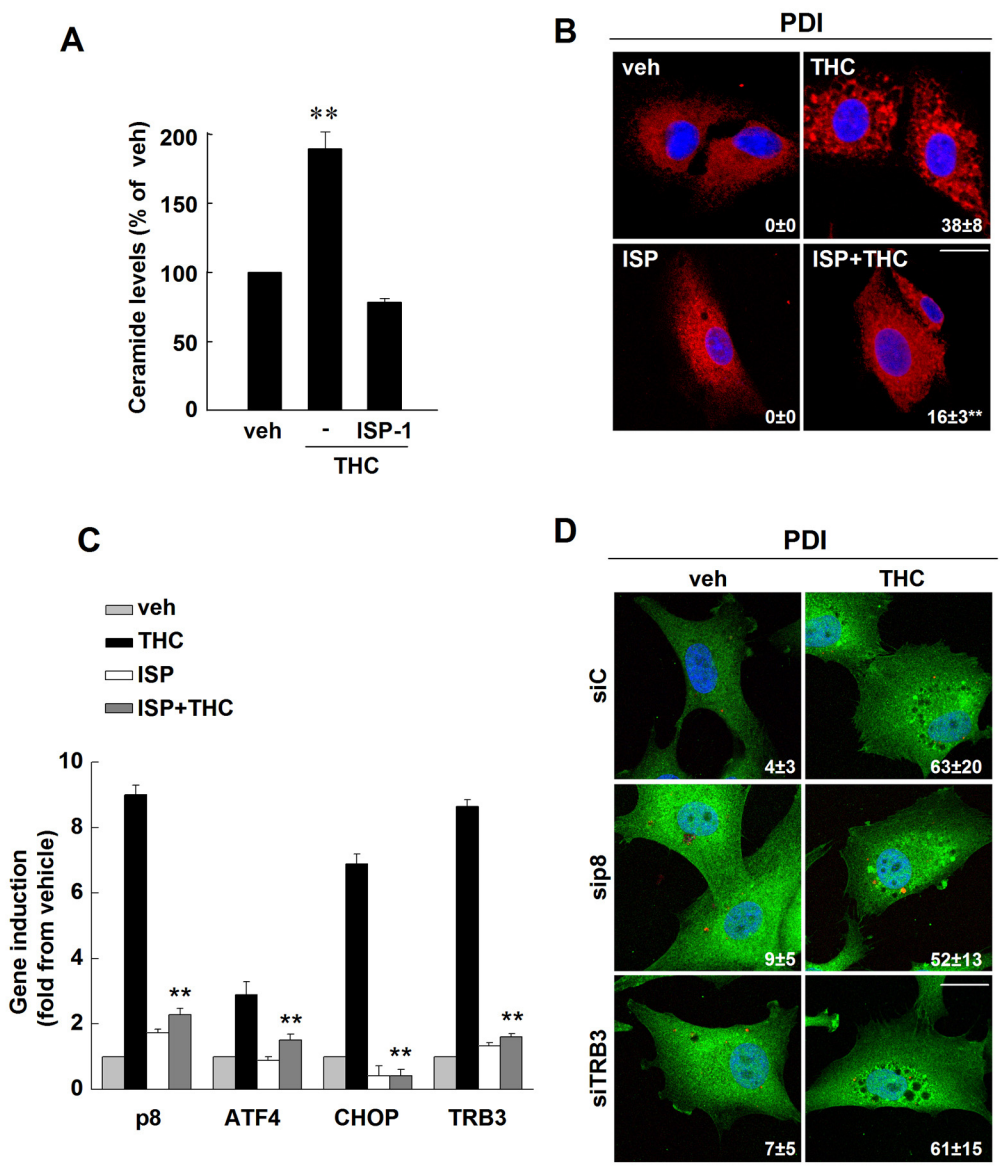

Supplemental Figure 4
Inhibition of ceramide biosynthesis but not knock-down of p8 or TRB3 prevents THC-induced ER dilation. (**A**) Effect of THC (8 h) on ceramide levels of U87MG cells pre-incubated with vehicle or ISP-1 (1 μM) (mean ± s.d.; n = 3; $^{**}P < 0.01$ from vehicle-treated cells). (**B**) Effect of THC on PDI immunostaining (red) of U87MG cells preincubated with ISP-1 (1 μM) (6 h; n = 3). Values represent the percentage of cells with PDI dots relative to the total number of cells (mean ± s.d.; n = 3; $^{**}P < 0.01$ from THC-treated cells). Bar: 20 μm. (**C**) Effect of THC (8 h) on p8, ATF-4, CHOP and TRB3 mRNA levels of U87MG pre-treated with vehicle or ISP-1 (1 μM). Data are expressed as the mean fold-increase ± s.d. relative to vehicle-treated cells. (n = 6; $^{**}P < 0.01$ from THC-treated cells). (**D**) Effect of THC (8 h) on PDI immunostaining (green) of U87MG cells transfected with control (siC), p8 (sip8) or TRB3 (siTRB3) -selective siRNA. Values represent the percentage of cells with PDI dots relative to the total number of transfected cells (as determined by co-transfection with a red fluorescent control siRNA) (mean ± s.d.; n = 4). Bar: 20 μm.

Salazar et al. Supplemental Figure 5

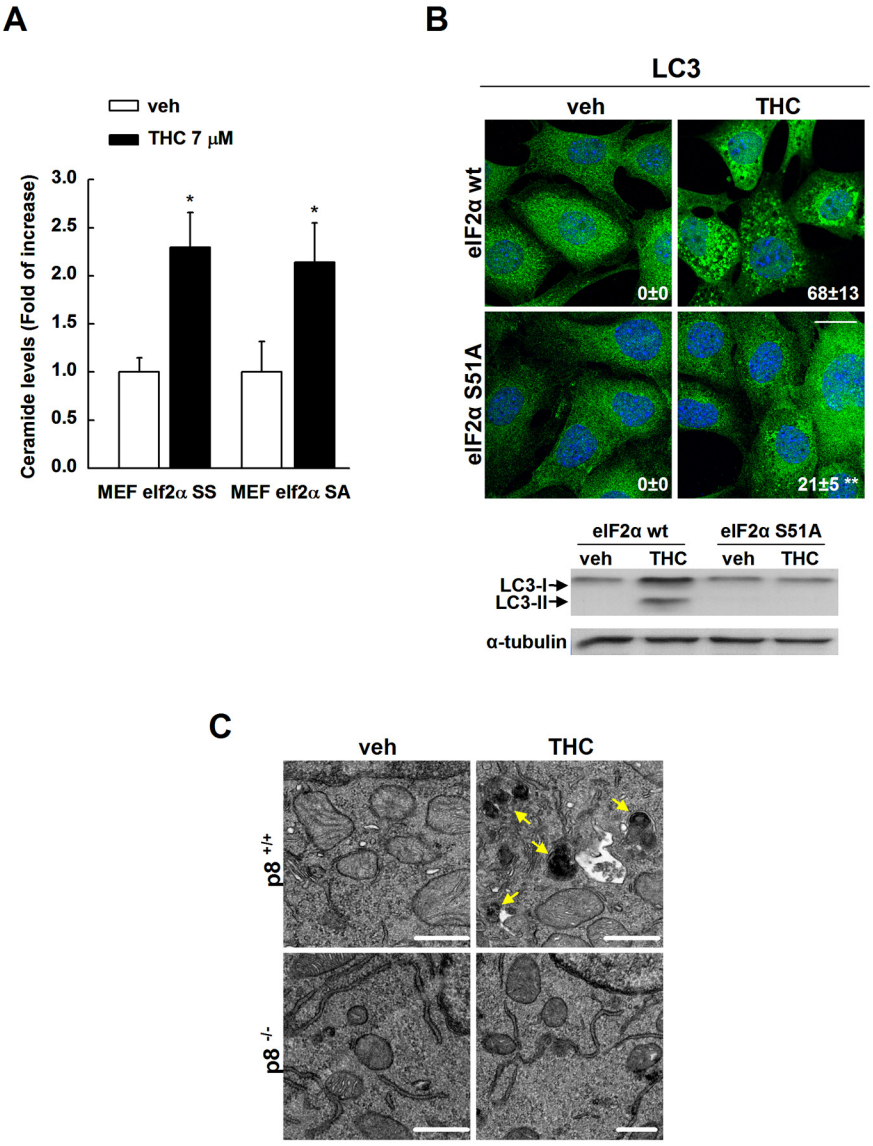

Supplemental Figure 5
eIF2α S51A and p8$^{-/-}$ MEFs are resistant to THC-induced autophagy. (**A**) Effect of THC (8 h) on ceramide levels of eIF2α wt and S51A MEFs. (mean ± s.d.; n = 3; *P < 0.05 from vehicle-treated cells) (**B**) Upper panel: Effect of THC (18 h) on LC3 immunostaining of eIF2α wt and S51A MEFs. Values represent the percentage of cells with LC3 dots relative to the total number of cells (mean ± s.d.; n = 4; **P < 0.01 from THC-treated eIF2α wt MEFs). Bar: 20 μm. Lower panel: Effect of THC (18 h) on LC3 lipidation of eIF2α wt and S51A MEFs (n = 3). (**C**) Effect of THC (6 h) on p8$^{+/+}$ and p8$^{-/-}$ MEFs. Representative electron microscopy photomicrographs are shown. Note the presence of late autophagosomes in p8$^{+/+}$ THC but not vehicle (veh)-treated cells (arrows). Bars: 500 nm.

Salazar et al. Supplemental Figure 6

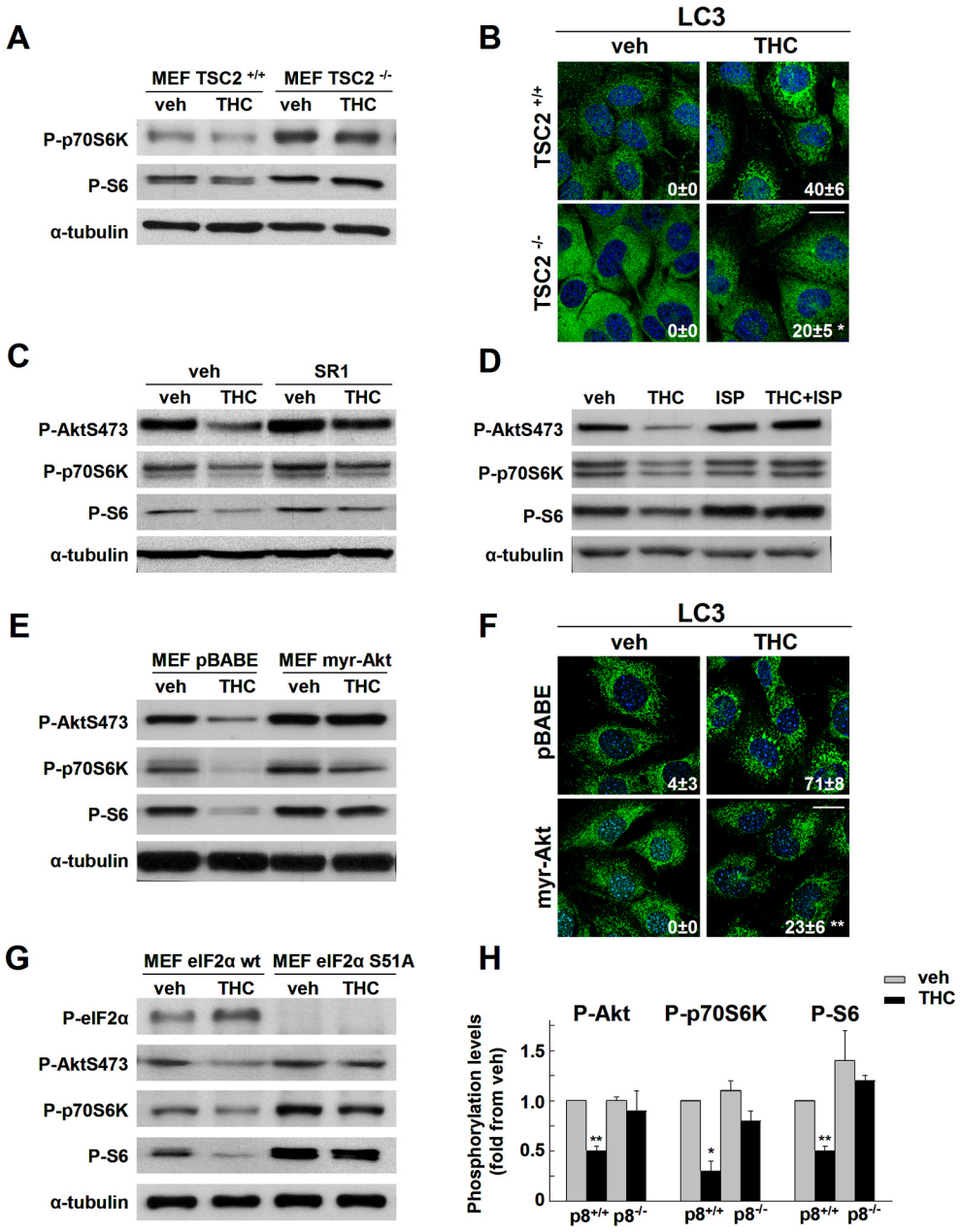

Supplemental Figure 6

TSC2$^{-/-}$, myr-Akt, eIF2α S51A and p8$^{-/-}$ MEFs as well as SR1- or ISP-1-treated U87MG cells are resistant to THC-induced mTORC1 inhibition. (**A**) Effect of THC (18 h) on p70S6k and S6 phosphorylation of TSC2$^{+/+}$ and TSC2$^{-/-}$ MEFs (n = 3). (**B**) Effect of THC (18 h) on LC3 immunostaining of TSC2$^{+/+}$ and TSC2$^{-/-}$ MEFs. Values represent the percentage of cells with LC3 dots relative to the total number of cells (mean ± s.d.; n = 3; $^{**}P < 0.01$ from THC-treated TSC2$^{+/+}$ MEFs). Bar: 20 μm. (**C**) Effect of THC (18 h) on Akt, p70S6k and S6 phosphorylation of U87MG cells pre-incubated with vehicle or SR1 (1 μM; n = 3). (**D**) Effect of THC (18 h) on Akt, p70S6k and S6 phosphorylation of U87MG cells pre-incubated with vehicle or ISP-1 (1 μM; n = 3). (**E**) Effect of THC (18 h) on Akt, p70S6k and S6 phosphorylation of pBABE and myr-Akt MEFs (n = 4). (**F**) Effect of THC (18 h) on LC3 immunostaining of pBABE and myr-Akt MEFs. Values represent the percentage of cells with LC3 dots relative to the total number of cells (mean ± s.d.; n = 3; $^{**}P < 0.01$ from THC-treated pBABE MEFs). Bar: 20 μm. (**G**) Effect of THC on eIF2α (3 h), Akt, p70S6k and S6 (18 h) phosphorylation of eIF2α wt and S51A MEFs (n = 5). (**H**) Effect of THC (18 h) on Akt, p70S6k and S6 phosphorylation of p8$^{+/+}$ and p8$^{-/-}$. Data represent the optical density values relative to vehicle-treated p8$^{+/+}$ MEFs (mean ± s.d.; n = 7; $^{*}P < 0.05$ or $^{**}P < 0.01$ from vehicle-treated p8$^{+/+}$ MEFs).

Salazar et al. Supplemental Figure 7

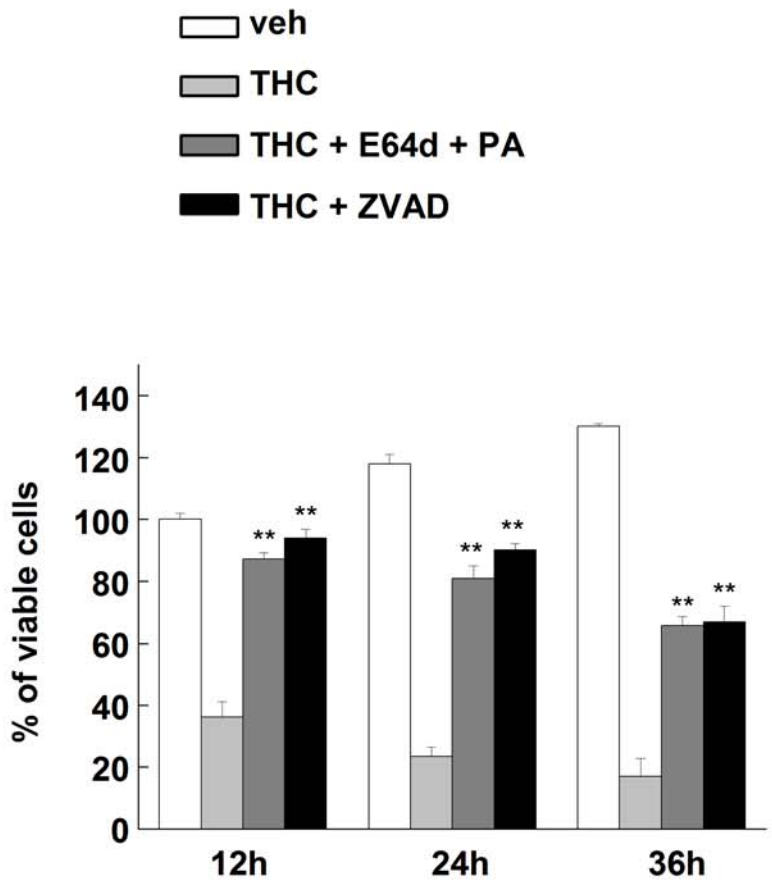

Supplemental Figure 7
Pharmacological inhibition of autophagy or apoptosis prevents THC-induced cell death. Effect of THC on the viability of U87MG cells pre-incubated with vehicle, E64d + pepstatine A (PA) (10 μM + 10 μg/ml) or ZVAD (10 μM) (mean ± s.d.; n = 3; $^{**}P < 0.01$ from THC-treated cells). Data are expressed as the percentage of viable cells relative to 12 h vehicle-treated cells.

Salazar et al. Supplemental Figure 8

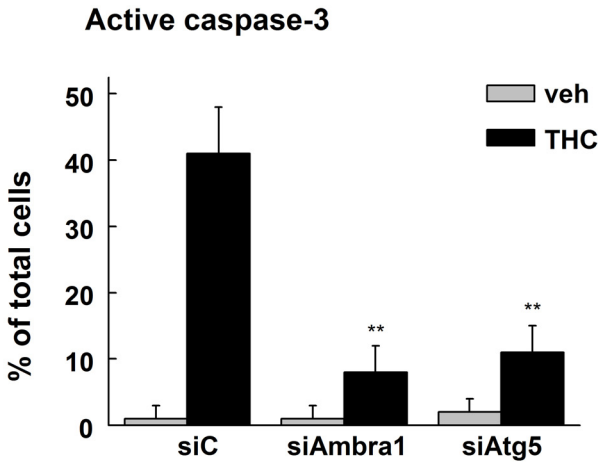

Supplemental Figure 8
Genetic inhibition of autophagy prevents THC-induced apoptosis. Effect of THC (24 h) on active caspase-3 immunostaining of U87MG cells transfected with siC, siAmbra1 or siAtg5. Data represent the percentage of active caspase-3 positive cells relative to the total number of transfected cells (as determined by co-transfection with a red fluorescent control siRNA) (mean ± s.d.; n = 3; $^{**}P < 0.01$ from THC-treated siC-transfected cells).

Salazar et al. Supplemental Figure 9

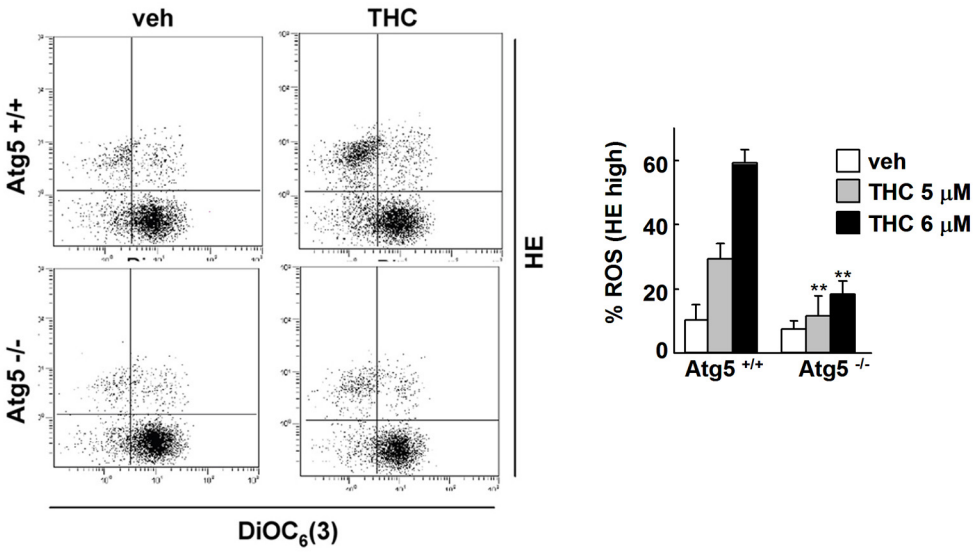

Supplemental Figure 9
Autophagy is upstream of apoptosis in THC-induced cell death. Effect of THC (24 h) on loss of mitochondrial membrane potential and ROS production of $Atg5^{+/+}$ and $Atg5^{-/-}$ MEFs as determined by $DIOC_6(3)$ and HE cytofluorometric analysis. A representative dot plot experiment is shown. Data represent the percentage of cells with high HE staining (mean ± s.d; n = 4, $^{**}P < 0.01$, from THC-treated $Atg5^{+/+}$ MEFs).

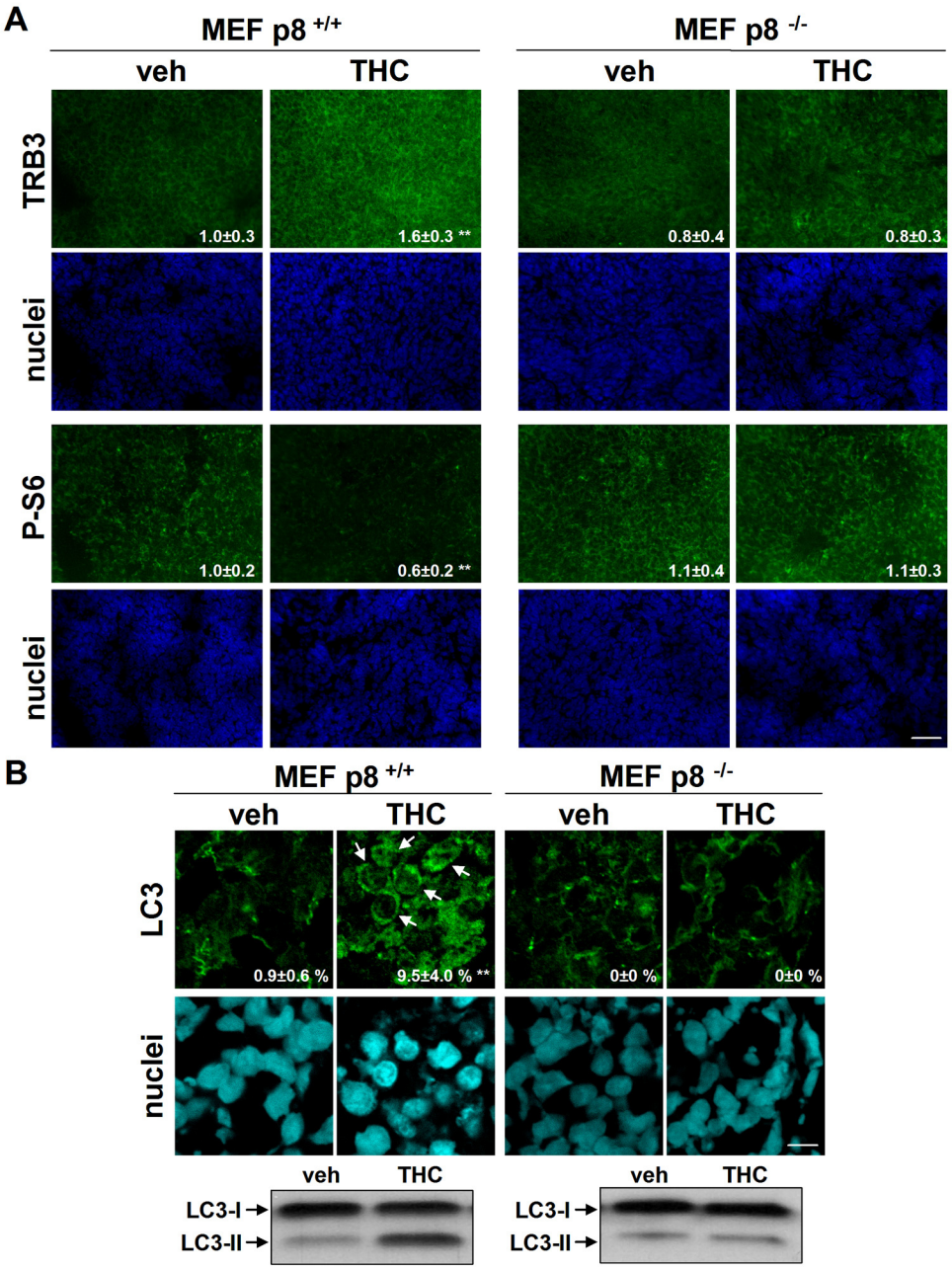

Supplemental Figure 10

THC activates the autophagy-mediated cell death pathway in $p8^{+/+}$ but not $p8^{-/-}$ xenografts. (**A**) Effect of THC administration on TRB3 and phospho-S6 immunostaining of Ras^{V12}/E1A-$p8^{+/+}$ and $p8^{-/-}$ tumor xenografts. Representative images of TRB3 and phospho-S6 immunostaining are shown. Values correspond to TRB3 or phospho-S6-stained area normalized to the total number of nuclei in each section and are expressed as the mean fold change ± s.d relative to vehicle-treated $p8^{+/+}$ tumors (18 sections for each of 3 dissected tumors for each condition were counted; $^{**}P < 0.01$ from vehicle-treated $p8^{+/+}$ tumors). Bar: 50 μm. (**B**) Upper panel: Effect of THC administration on LC3 immunostaining of Ras^{V12}/E1A-$p8^{+/+}$ and $p8^{-/-}$ tumor xenografts. Representative images of vehicle and THC-treated tumors are shown. Arrows point to cells with LC3 dots. Values correspond to the percentage of cells with LC3 dots relative to the total number of nuclei in each section ± s.d (10 sections for each of 3 dissected tumors for each condition were counted; $^{**}P < 0.01$ from vehicle-treated tumors). Bar: 20 μm. Lower panel: Effect of THC administration on LC3 lipidation of Ras^{V12}/E1A-$p8^{+/+}$ and $p8^{-/-}$ tumor xenografts. Representative samples from one vehicle and one THC-treated $p8^{+/+}$ and $p8^{-/-}$ tumors are shown.

Salazar et al. Supplemental Figure 10 (cont)

C

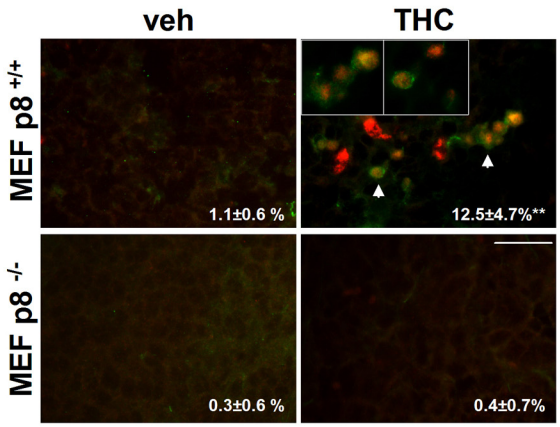

Supplemental Figure 10 (cont)
THC activates the autophagy-mediated cell death pathway in $p8^{+/+}$ but not $p8^{-/-}$ xenografts. (**C**) Effect of THC administration on active caspase-3 (red) and LC3 (green) immunostaining in Ras^{V12}/E1A-$p8^{+/+}$ and $p8^{-/-}$ MEF-tumor xenografts. Representative images from one vehicle and one THC-treated $p8^{+/+}$ and $p8^{-/-}$ tumors are shown. Values correspond to 10 sections of 3 dissected tumors for each condition and are expressed as the percentage of active caspase-3-positive cells relative to the total number of nuclei in each section (**$P < 0.01$ from vehicle-treated tumors). Bars: 20 μm.

Salazar et al. Supplemental Figure 11

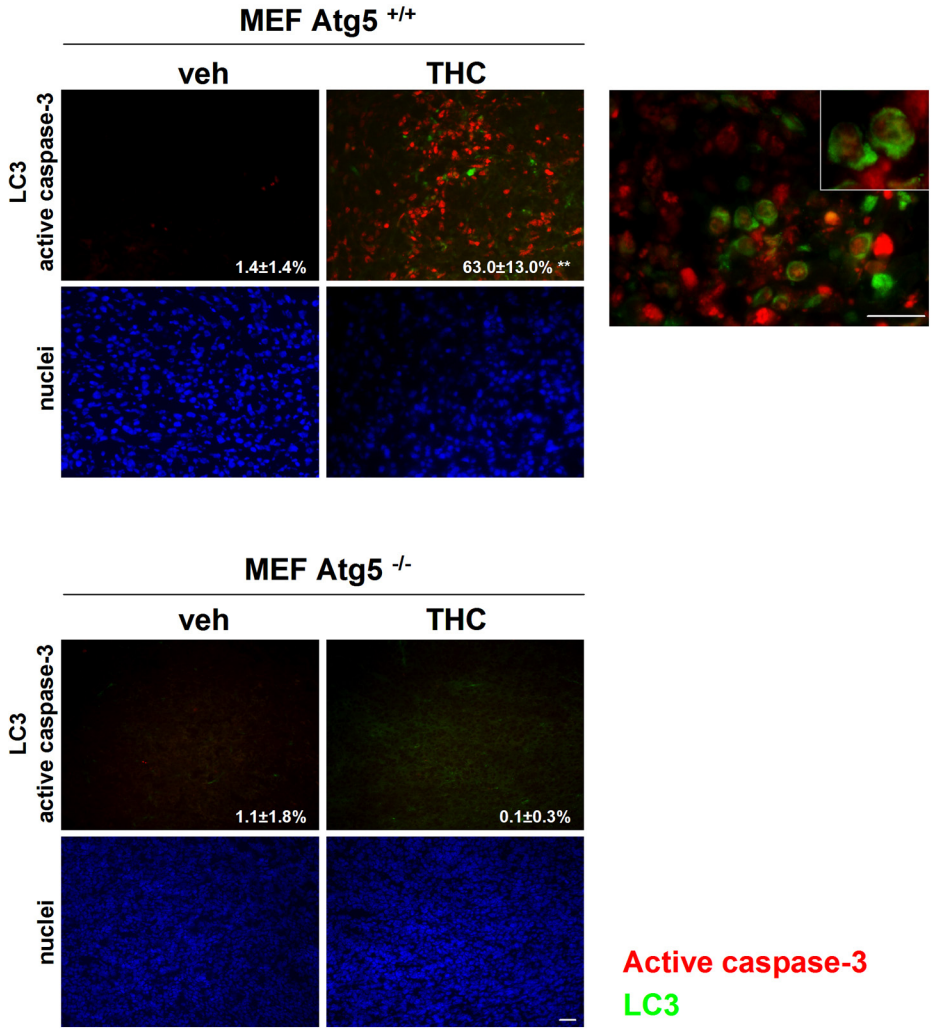

Supplemental Figure 11
THC activates the autophagy-mediated cell death pathway in $Atg5^{+/+}$ but not $Atg5^{-/-}$ xenografts. Effect of THC administration on active caspase-3 (red) and LC3 (green) immunostaining in T-large antigen/Ras^{V12}-$Atg5^{+/+}$ and $Atg5^{-/-}$ MEF-tumor xenografts. Representative images from one vehicle and one THC-treated $Atg5^{+/+}$ and $Atg5^{-/-}$ tumors are shown. A high magnification photomicrograph of a THC-treated $Atg5^{+/+}$ tumor is included (right panel). Values correspond to 10 sections of 3 dissected tumors for each condition and are expressed as the percentage of active caspase-3-positive cells relative to the total number of nuclei (**$P < 0.01$ from vehicle-treated tumors). Bars: 20 μm